Front. Med. 2021, 15(6): 922–932
https://doi.org/10.1007/s11684-020-0804-7

RESEARCH ARTICLE

Orlistat induces ferroptosis-like cell death of lung cancer cells

Wenjing Zhou[1], Jing Zhang[3], Mingkun Yan[4], Jin Wu[1], Shuo Lian[4], Kang Sun[1], Baiqing Li[5], Jia Ma[2], Jun Xia (✉)[2], Chaoqun Lian (✉)[2]

[1]Research Center of Clinical Laboratory Science, Bengbu Medical College, Bengbu 233030, China; [2]Department of Biochemistry and Molecular Biology, School of Laboratory Medicine, Bengbu Medical College, Bengbu 233030, China; [3]Department of Genetics, School of Life Sciences, Bengbu Medical College, Bengbu 233000, China; [4]Department of Clinical Medicine, Bengbu Medical College, Bengbu 233000, China; [5]Anhui Key Laboratory of Infection and Immunity, Bengbu Medical College, Bengbu 233030, China

Abstract **Aberrant *de novo* lipid synthesis is involved in the progression and treatment resistance of many types of cancers, including lung cancer; however, targeting the lipogenetic pathways for cancer therapy remains an unmet clinical need. In this study, we tested the anticancer activity of orlistat, an FDA-approved anti-obesity drug, in human and mouse cancer cells *in vitro* and *in vivo*, and we found that orlistat, as a single agent, inhibited the proliferation and viabilities of lung cancer cells and induced ferroptosis-like cell death *in vitro*. Mechanistically, we found that orlistat reduced the expression of GPX4, a central ferroptosis regulator, and induced lipid peroxidation. In addition, we systemically analyzed the genome-wide gene expression changes affected by orlistat treatment using RNA-seq and identified FAF2, a molecule regulating the lipid droplet homeostasis, as a novel target of orlistat. Moreover, in a mouse xenograft model, orlistat significantly inhibited tumor growth and reduced the tumor volumes compared with vehicle control ($P < 0.05$). Our study showed a novel mechanism of the anticancer activity of orlistat and provided the rationale for repurposing this drug for the treatment of lung cancer and other types of cancer.**

Keywords orlistat; ferroptosis; FAF2; lung cancer

Introduction

Significant advances have been made in the diagnosis and treatment of lung cancer; however, lung cancer remains as the leading cause of cancer-related death worldwide, with an estimate of 1.8 million lung cancer deaths each year [1]. Therefore, effective therapies are needed for this fatal disease. Recent studies have found that the lipogenic pathway plays an important role in lung cancer progression and treatment resistance [2–4], and agents targeting this pathway have shown some preclinical efficacies [5,6]. However, developing effective agents targeting the lipogenetic pathway for cancer therapy remains an unmet clinical need.

Orlistat is a potent inhibitor of gastric and pancreatic lipase, and it can reduce dietary fat uptake [7,8]. It has been approved by the US Food and Drug Administration (FDA) for the treatment of obesity [8]. The targets of orlistat are not specific, and orlistat has also been shown to inhibit the activity of fatty acid synthase (FASN), a key enzyme for *de novo* lipid synthesis [9]. Orlistat has been previously tested as a FASN inhibitor in several types of cancer cells, which inhibits cancer cell proliferation and metastasis in animal models [10–15]. Recent studies also showed that orlistat impaired cell growth and downregulated PD-L1 expression in human T cell leukemia cell line [16], and it also inhibited metastasis in mouse melanoma model possibly through increasing the populations of dendritic cells, natural killer cells, and CD8 T lymphocytes [14], indicating that the multiple mechanisms and targets could be involved in the anticancer activity of orlistat. However, systemic analysis of the targets of orlistat has not been performed, and its potential anticancer activity in lung cancer models is unknown.

In this study, we tested the anticancer activity of orlistat in human and mouse lung cancer cell lines *in vitro* and *in vivo* and analyzed the genome-wide gene expression

Received March 27, 2020; accepted May 20, 2020
Correspondence: Jun Xia, xiajunbbmu@126.com;
Chaoqun Lian, lianchaoqun@bbmc.edu.cn

changes using the RNA-seq method. We found that orlistat inhibited the proliferation and induced ferroptosis-like cell death of lung cancer cells *in vitro* and inhibited tumor growth *in vivo*. In addition, orlistat inhibited lipid peroxidation and reduced the protein level of glutathione peroxidase 4 (GPX4), a ferroptosis regulator. We also identified FAS-associated factor 2 (FAF2) as a novel orlistat target, which might be partially involved in the anticancer activity mediated by orlistat treatment.

Materials and methods

Reagents

MTT (3-(4,5-dimethyl-2-thiazolyl)-2,5-diphenyl2-H-tetrazolium bromide) was bought from Sigma-Aldrich (St. Louis, MO, USA). Orlistat was purchased from Selleck Chemicals (Shanghai, China). Annexin V-FITC/PI apoptosis assay kit was purchased from BD Biosciences. C_{11}-BODIPY581/591 (D3861) probe was purchased from Invitrogen™. Antibodies for PARP (Cat#: 9532), p-ERK1/2 (Cat#: 4370), Vinculin (Cat#:13901), and secondary antibodies were obtained from Cell Signaling Technology. Antibodies for GPX4 (GTX65845) and FAF2 (GTX115680) were purchased from GeneTex.

Cell lines and cell culture

Human NSCLC lines H1299, A549, and mouse lung cancer cell line LLC were purchased from the Chinese Academy of Sciences Cell Bank (Shanghai, China). H1299 and A549 cells were cultured in RPMI-1640 medium (Gibco, Gaithersburg, MD, USA) supplemented with 10% fetal bovine serum (FBS) in 5% CO_2 at 37 °C. LLC cells were cultured in DMEM medium (Gibco) supplemented with 10% FBS with 5% CO_2 at 37 °C.

Cell viability assay

H1299, A549, and LLC cells were cultured in 96-well plates (3×10^3 cells/well) overnight, and cells were treated with different concentrations of orlistat for 72 h. Cell proliferation was assessed by MTT assay. Each value was normalized by the readings from the cells treated with DMSO. Independent experiments were performed three times.

Colony formation assay

H1299, A549, and LLC cells were seeded in 6-well plates (1×10^3 cells/well) and incubated overnight. Then, cells were treated with different concentrations of orlistat. Plates were placed at 37 °C, 5% CO_2, for 1 week. After fixation with paraformaldehyde for 15 min, cells were stained with crystal violet for 15 min and then placed under a microscope to count the number of clones with over 50 cells.

Flow cytometry assay

H1299, A549, and LLC cells were seeded in a 6-well plate (3×10^5 cells/well) and incubated overnight. Then, cells were treated with various concentrations of orlistat for 36 h. Cells were harvested and washed with PBS and resuspended in 5 mL binding buffer containing annexin V-FITC/PI. Fluorescence-activated cell sorting was performed to analyze cell death and apoptosis.

Western blotting

Cells were lysed using RIPA buffer supplemented with protease inhibitor cocktail. The protein concentrations were measured using a BCA protein assay. Proteins (60 μg) were separated using 10% SDS-PAGE and transferred onto PVDF membranes. The membranes were blocked with 5% non-fat milk in TBST (TBS with Tween) at room temperature for 2 h, followed by incubation with primary antibodies overnight at 4 °C. The membranes were rinsed with TBST three times and then incubated with secondary antibody for 1 h at room temperature. The results were visualized with the enhanced chemiluminescence.

Lipid peroxidation assay with the fluorescent probe C_{11}-BODIPY581/591

H1299 and A549 cells were cultured in a 6-well plate (2×10^5 cells/well) overnight and then treated with various concentrations of orlistat for 24 h. C_{11}-BODIPY581/591 was dissolved in DMSO to make a 5 mmol/L stock solution, and 25 μL was added into each well. Then, the plate was returned to a tissue culture incubator for 20 min. The plate was removed and washed with PBS, and images were acquired with a Zeiss Axio Observer fluorescence microscope.

RNA-seq and data analysis

Cells were treated with 30 μmol/L of orlistat for 48 h. Then, total RNA was prepared using TRIzol (Invitrogen). cDNA library construction and RNA-seq analysis were performed at the Jiema DNA Biotech Company (Shanghai, China). In brief, mRNA was enriched from total RNA using Dynal magnetic beads (Invitrogen) and fragmented (approximately 200 bp) with alkaline hydrolysis (Ambion). Library was prepared and sequenced using an Illumina machine. STAR v2.5 was used to map the data in mouse genome (10 mm) with mismatch = 2. Read numbers for each gene were counted using HTSeq v 0.6.1. Differential gene expression analysis between the control

and treatment groups was conducted using DESeq2 R package (v 2_1.6.3) to generate fold changes (FC), *P* value, and false discovery rate (FDR = 0.05) adjusted *P* values. Significantly differential expressed genes (adjusted $P < 0.05$) and associated signaling pathways were annotated with the online program ENRICHR.

Real-time polymerase chain reaction (PCR) analysis

Cells were treated with orlistat for 48 h, and then total RNA was isolated with TRIzol reagent. Total RNA (2 μg) was used for reverse transcription with cDNA synthesis kit (Invitrogen). Real-time PCR primers for human *FAF2* and *GAPDH* (internal control) genes were purchased from Bio-Rad. Real-time PCR was performed with iQ SYBR Green Supermix (Bio-Rad) on a CFX96 real-time PCR machine (Bio-Rad).

Gene knockdown and overexpression

Cells (5×10^5) were grown in 6-well plates for 24 h and transfected with pcDNA-FAF2, FAF2-siRNA, or empty vector using Lipofectamine 2000 (Invitrogen), according to the manufacturer's instructions. siRNA-FAF2 (5′-CAUUCCGGUUUACCUAUUTT-3′; 5′-AAUAG-GUAAACCGGAAUGGTT-3′), siRNA-Control, pcDNA-FAF2, and pcDNA3.1 vector were purchased from GenePharma (Shanghai, China).

In vivo experiments

C57BL/6 mice were anesthetized, and 5×10^5 LLC cells were implanted subcutaneously into the right flank. Five days post-implant, mice were randomized and assigned into two groups and treated with orlistat (10 mg/kg, intraperitoneal injection) or PBS daily for 14 days. The tumor volume was measured twice a week with a caliper, and the tumor volume was calculated according to the formula ((length × width^2)/2). On the 22nd day, all mice were sacrificed, and the tumors were removed and weighed. The animal studies and procedures were approved by the Institutional Animal Care and Use Committee at Bengbu Medical College.

Immunohistochemistry (IHC) staining

IHC staining was performed by using the horseradish peroxidase (HRP) method (Vector Laboratories). In brief, after antigen-retrieval procedure, tissue slides were washed with PBS, blocked with 3% BSA for 1 h at room temperature, and then stained with antibodies against FAF2 (1:100; GTX07993, GeneTex), followed by incubation with HRP-conjugated second antibody. The results were visualized with 3,3-diaminobenzidine (DAB).

Statistical analyses

All data were analyzed using GraphPad Prism 8.0 software (California Corporation). The results were expressed as the mean ± SD. Differences between each group of values and its control were evaluated by Student's *t*-test. $P < 0.05$ was considered statistically significant.

Results

Orlistat inhibited lung cancer cell proliferation

Orlistat is a lipase inhibitor approved for the treatment of obesity, and evidence has shown that it can also inhibit FASN activity, thereby inhibiting the cellular lipogenic pathway. We tested the anticancer activity of orlistat using MTT and colony formation assay with three lung cancer cell lines (A549, H1299, and LLC) to investigate whether orlistat has therapeutic potential for lung cancer. The results showed that cell growths were significantly inhibited by orlistat in a dose-dependent manner in all three cell lines. In particular, we found that 30 μmol/L of orlistat suppressed cell growth by 50%–75% (Fig. 1A). In colony formation assay, orlistat significantly inhibited colony numbers at the doses of 10–100 μmol/L (Fig. 1B and 1C). These results indicated that orlistat inhibited the proliferation of lung cancer cells.

Orlistat induced ferroptosis-related cell death

We treated the cells with different doses of orlistat for 36 h to test if orlistat could induce apoptosis or cell death, and then cell death and apoptosis were measured by annexin V-FITC/PI assay using flow cytometry. The results showed that orlistat induced dramatic cell death and apoptosis of A549, H1299, and LLC cells (Fig. 2A–2C). Using Western blotting, we tried to determine whether orlistat could induce cleaved PARP, an apoptotic marker. However, no cleaved PARP was detected in orlistat-treated A549 or H1299 cells, indicating that orlistat-induced cell death might not be mediated by the classical apoptotic pathway. Then, we checked the expression of GPX4, a key molecule in ferroptosis regulation, by inhibiting peroxidation, and the result showed that GPX4 was dramatically reduced by orlistat treatment. In addition, phosphor-ERK (p-ERK), which positively regulates ferroptosis, was upregulated by orlistat treatment in both cell lines (Fig. 2D). These results indicated that orlistat might induce ferroptosis-mediated cell death.

Orlistat induced lipid peroxidation

We used the C_{11}-BODIPY581/591 lipid probe to analyze lipid peroxidation, which is a marker for cell ferroptosis

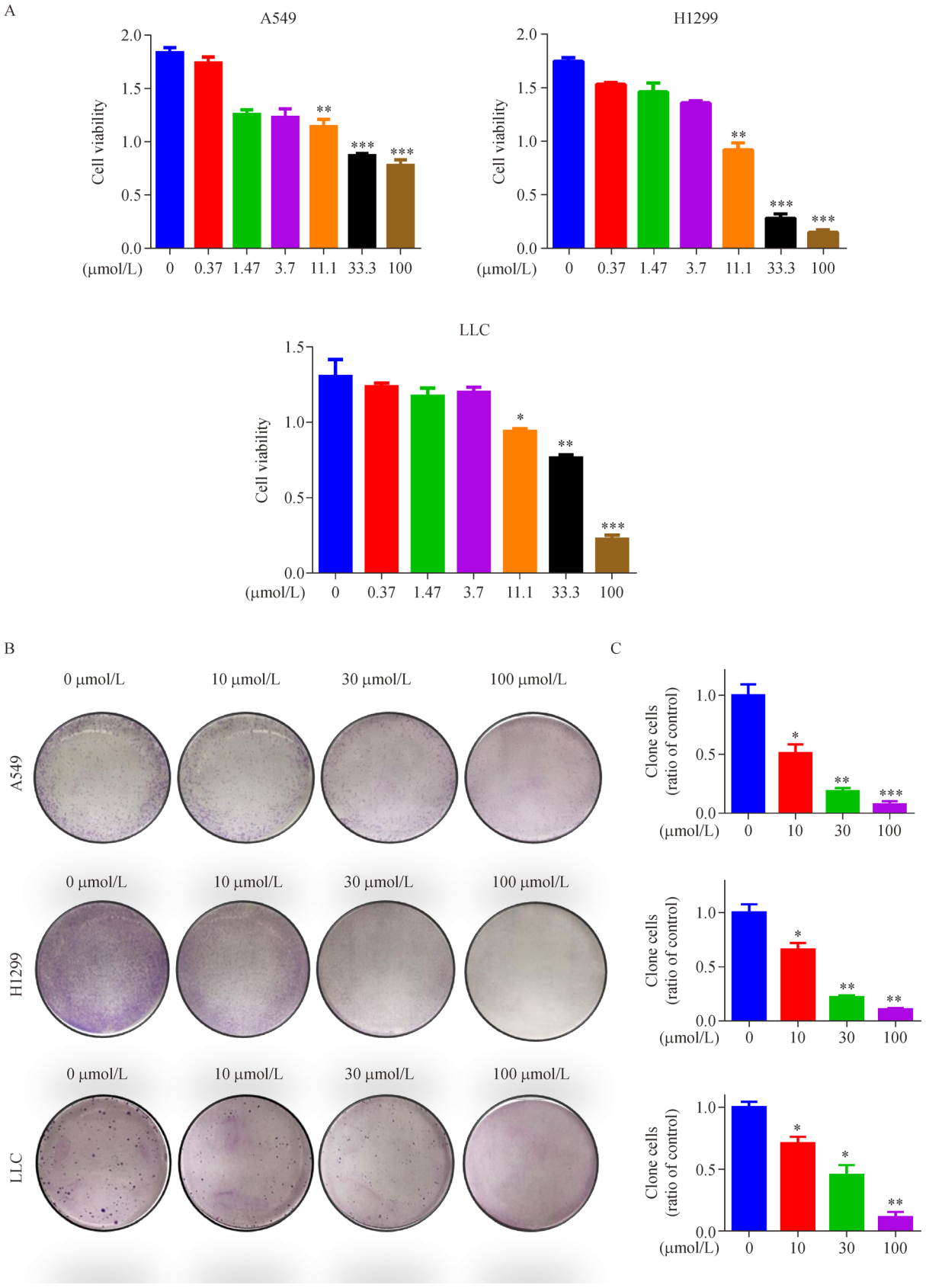

Fig. 1 Orlistat inhibits lung cancer cell proliferation. (A) Cell growth was measured with MTT assay after treatment with orlistat for 72 h. Data were represented as mean ± SD (* $P < 0.05$, ** $P < 0.01$, *** $P < 0.001$). (B and C) Colony formation assay: cells were treated with orlistat for 1 week, and cell colony was counted and analyzed. Data were represented as mean ± SD (*$P < 0.05$, **$P < 0.01$, ***$P < 0.001$).

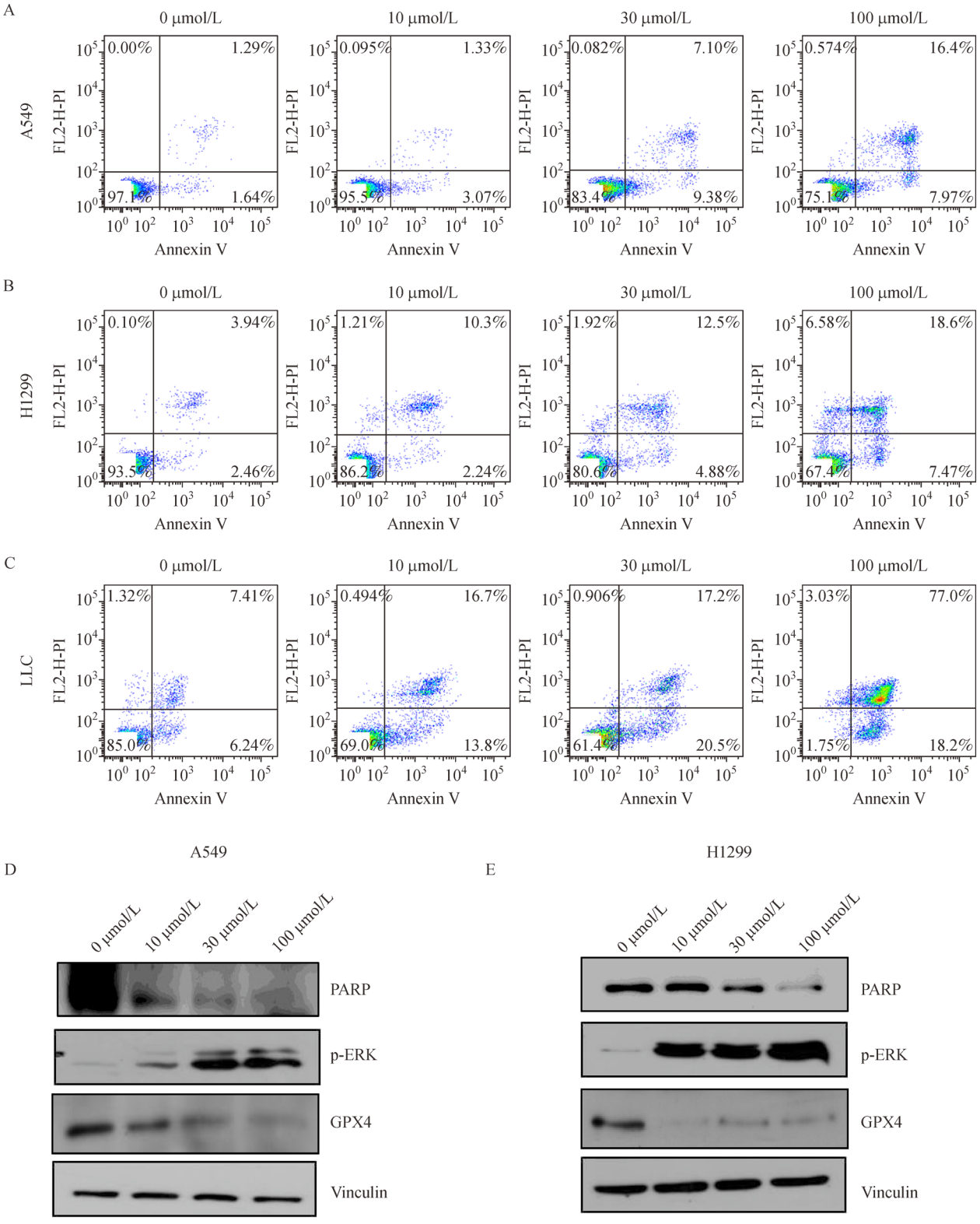

Fig. 2 Orlistat induced ferroptosis-like cell death. (A–C) Flow cytometry analysis of cell apoptosis in lung cancer cells with the annexin V-FITC/PI method after orlistat treatment for 36 h. (D and E) Western blotting analysis was conducted to measure the expression of PARP, p-ERK1/2, and GPX-4 after treatment with orlistat for 48 h.

[17]. C_{11}-BODIPY581/591 is normally used to measure antioxidant activity in the lipid environment, and it stains lipid membrane and displays red fluorescence when unoxidized lipid is present [17]. The fluorescence is lost upon interaction with peroxyl radicals, which are products from lipid peroxidation. The results showed that different doses of orlistat dramatically reduced the red fluorescence intensity (Fig. 3A and 3B), indicating that orlistat induced lipid peroxidation. In addition, we observed that C_{11}-BODIPY581/591-stained vesicles were reduced by orlistat treatment (Fig. 3A and 3B). These results further indicated that orlistat induced cell lipid peroxidation.

Genome-wide profiling of gene expression changes mediated by orlistat

We used RNA-seq to profile the genome-wide gene expression changes in LLC lung cancer cells after treatment with orlistat (30 μmol/L) for 24 h, understand the detailed mechanism of the anticancer activity of orlistat, and identify novel targets. With a false discovery rate of 5% and adjusted *P* value of 0.05, we identified 77 differential expressed genes (Fig. 4A). In addition, analysis of these genes with ENRICHR revealed that multiple pathways were inhibited by orlistat treatment, including proteasome-activating ATPase, lipase inhibitor activity, and RNA polymerase I/II activity, whereas the signaling pathways involved in mesenchymal–epithelial transition, endocytic recycling, and cellular response to cholesterol were upregulated (Fig. 4B and 4C). In particular, we found that FAF2 or UBX domain-containing protein 8 (UBXD8), a molecule regulating lipid droplet (LD) formation and homeostasis, was downregulated by orlistat treatment (Fig. 4A), indicating that FAF2 could be a novel target of orlistat. Using quantitative real-time PCR, we confirmed that FAF2 was downregulated in H1299 and A549 cells after treatment with different doses of orlistat (Fig. 4D). Moreover, downregulation of FAF2 by orlistat was validated with Western blotting in both cell lines (Fig. 4E). These results indicated that orlistat suppressed FAF2 expression in lung cancer cells.

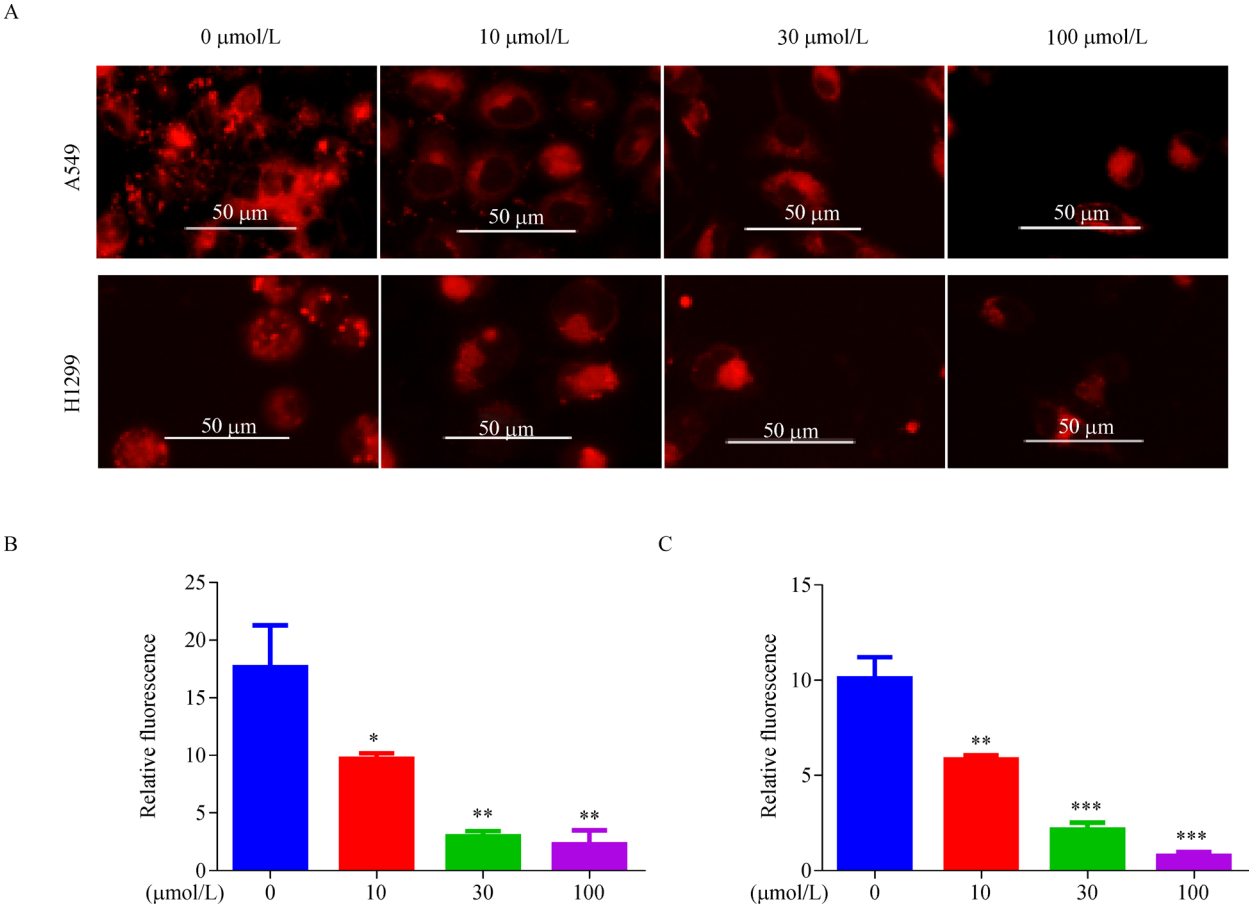

Fig. 3 Assessment of lipid peroxidization. (A) Cells were treated with different concentrations of orlistat and DMSO for 24 h; cells were stained with C_{11}-BODIPY581/591 to analyze lipid peroxidization under a fluorescence microscope, and representative images were shown. (B and C) Quantifications of fluorescence intensity. Data were represented as mean ± SD (*$P < 0.05$, **$P < 0.01$, ***$P < 0.001$).

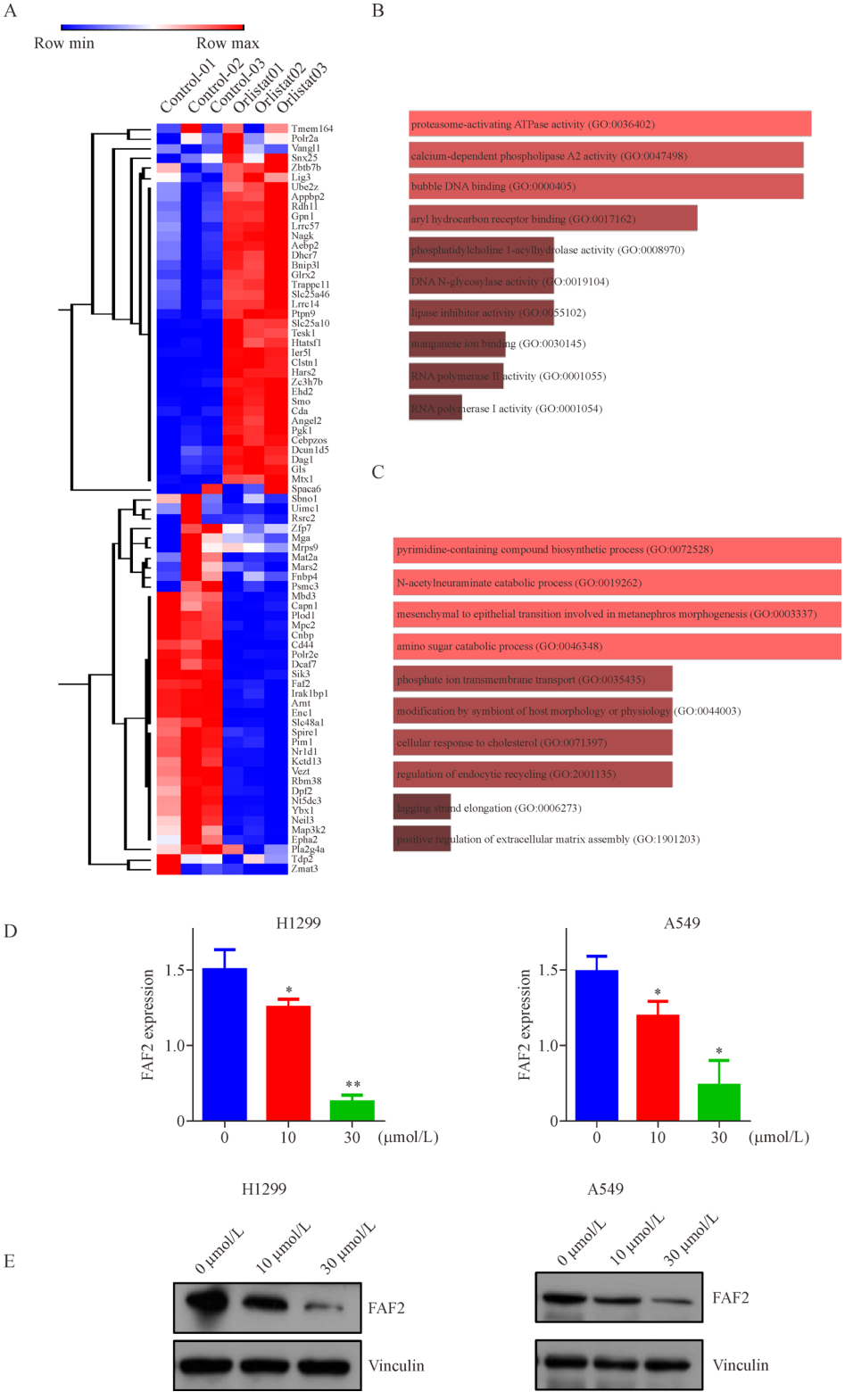

Fig. 4 Orlistat repressed the expression of FAF2. (A) RNA-seq analysis of the gene expression profile of LLC cells treated with orlistat for 48 h. Heatmap was generated with significantly up- and downregulated genes (FDR = 0.05 and $P < 0.05$). (B and C) Gene set enrichment analysis of up- and downregulated genes with online program ENRICHR. The pathways potentially affected by orlistat were shown. (D) Real-time PCR validation of FAF2 mRNA expression in H1299 and A549 cells treated with different concentrations of orlistat. (E) Western blotting analysis of FAF2 expression in H1299 and A549 cells treated with different concentrations of orlistat for 48 h.

Orlistat inhibited cancer cell growth through FAF2 downregulation

FAF2 is a LD-related factor regulating LD formation and trafficking. We knocked down FAF2 expression in H1299 and A549 cells to test if downregulation of FAF2 is involved in the viability inhibition of lung cancer cells induced by orlistat and then treated the cells with orlistat for 24 h to check cell viability (Fig. 5A and 5B). The result showed that the knockdown of FAF2 inhibited cell growth in H1299 and A549 cells (Fig. 5A and 5B), and the combination with 10 μmol/L of orlistat further decreased FAF2 expression and enhanced the viability inhibition. In addition, FAF2 was overexpressed through transient transfection of FAF2-expressing plasmid in A549 cells (Fig. 5E). Compared with the control vector, overexpression of FAF2 increased cell viability and rescued the inhibitory effects mediated by orlistat treatment (Fig. 5F). Our results indicated that downregulation of FAF2 was partially involved in orlistat-induced cell viability inhibition.

Orlistat inhibited tumor growth *in vivo*

We established a tumor model using the LLC lung cancer cell line, and the mice were treated with orlistat for 14 days to test its anticancer activity *in vivo*. The result showed that compared with the control, orlistat significantly inhibited tumor growth ($P < 0.001$; Fig. 6A). At the end of the experiment, the tumor sizes and tumor weights were reduced by 50% in the treatment group (Fig. 6B and 6C). IHC staining also confirmed that orlistat dramatically reduced FAF2 expression in the tumor tissues. This result indicated that orlistat, as a single treatment agent, had anticancer activity in the lung cancer model *in vivo*.

Discussion

Targeting the components of the cancer lipogenetic pathway has been actively explored for cancer therapies in preclinical models [9]. However, most of the FASN-targeting agents, including C75 and Tofa, have either low bioavailability or high toxicity, limiting their clinical use [18]. Orlistat, an FDA-approved drug for obesity treatment, inhibits FASN activity and documents clinical safety profile [9]. Therefore, further study of the anticancer activity and mechanism of action will facilitate repurposing of this drug for the treatment of multiple cancers with dysregulated lipogenetic activity, including lung cancers [4].

In this study, we showed that orlistat inhibited cell proliferation and viability in three lung cancer cell lines. In addition, using flow cytometry analysis, we revealed that orlistat induced apoptotic cell death; however, in Western blotting analysis, no cleaved PARP was detected in the cells treated with orlistat, although the total PARP expression levels were reduced by orlistat treatment in both H1299 and A549 cells, indicating that orlistat-induced cell death could be mediated by other mechanism. Previous study indicated that orlistat could induce lipid peroxidation in the rat brain [19], whereas lipid peroxidation could cause the cell ferroptosis pathway, a regulated cell death pathway mediated by iron ions or iron-containing enzymes [20]. Whether orlistat could induce ferroptosis has never been described. GPX4 is a central molecule regulating ferroptosis through neutralizing lipid peroxides [20]. Depletion of GPX4 in cancer cells could directly trigger ferroptosis [21,22]. A previous study has also shown that the activation of the MAPK pathway is involved in cell ferroptosis mediated by reactive oxygen species, whereas blocking MAPK protected the lung cancer cells from ferroptosis [23]. In our study, orlistat dramatically inhibited GPX4 expression and upregulated phosphorylated MAPK/ERK (Fig. 2B). In addition, orlistat induced lipid peroxidation in H1299 and A549 cells (Fig. 3A). These results were aligned with the characteristics of ferroptosis-mediated cell death, indicating that orlistat-induced viability inhibition and cell death could be mediated by ferroptosis.

In this study, we explored the genome-wide gene expression profile changes mediated by orlistat treatment using RNA-seq. Among the many significantly affected genes, we found that FAF2/UBXD8 was a novel target associated with lipid metabolism. The major role of FAF2 is to regulate the formation and trafficking of LD, whereas its roles in cancer have not been reported, although one recent report showed that it could be a biomarker for melanoma metastasis [24]. In our study, we found that the knockdown of FAF2 further enhanced the viability inhibition induced by orlistat, whereas, overexpression of FAF2 did the opposite. Our results indicated that the downregulation of FAF2 could be partially involved in orlistat-mediated anticancer activity. Nevertheless, the underlying mechanism of FAF2 inhibition by orlistat remained to be further explored, and whether inhibition of FAF2 caused lipid peroxidation and ferroptosis also needed to be determined in future studies.

We showed that orlistat inhibited the viability and induced ferroptosis-like cell death of lung cancer cells, and for the first time, we found that orlistat reduced the expression of GPX4, a key molecule regulating cell ferroptosis. Moreover, we analyzed the gene expression profile affected by orlistat and identified a novel orlistat target, FAF2, which might be involved in orlistat-mediated anticancer activity. This study might facilitate clinical translation of orlistat as a repurposed drug for the treatment of lung cancers and many other types of cancer with dysregulated lipogenetic pathways.

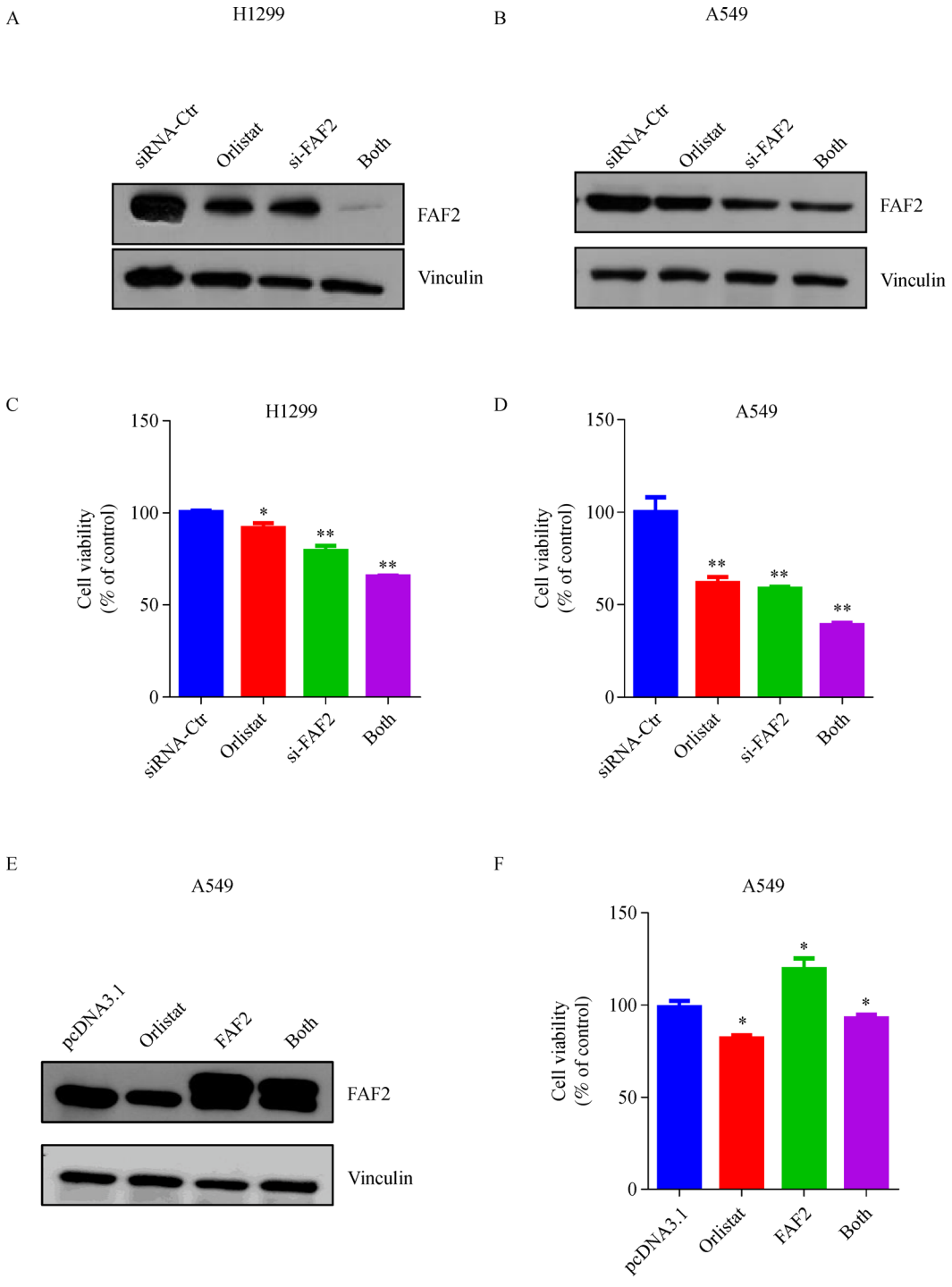

Fig. 5 Knockdown or overexpression of FAF2 affected cell proliferation. (A and B) Western blotting analysis of FAF2 expression in H1299 and A459 cells treated with 10 μmol/L of orlistat, transfected with control siRNA (siRNA-Ctr) or FAF2 siRNA (si-FAF2), or combination. (C and D) Cell viability assay with H1299 and A549 treated with 10 μmol/L of orlistat, si-FAF2, or combination for 48 h. Data were represented as mean ± SD (*$P < 0.05$, **$P < 0.01$). (E) Western blotting analysis of FAF2 expression in A549 cells treated with 10 μmol/L of orlistat, overexpression of FAF2, or combination. (F) Cell viability assay with A549 cells treated with 10 μmol/L of orlistat, overexpression of FAF2, or combination for 48 h. Data were represented as mean ± SD (*$P < 0.05$).

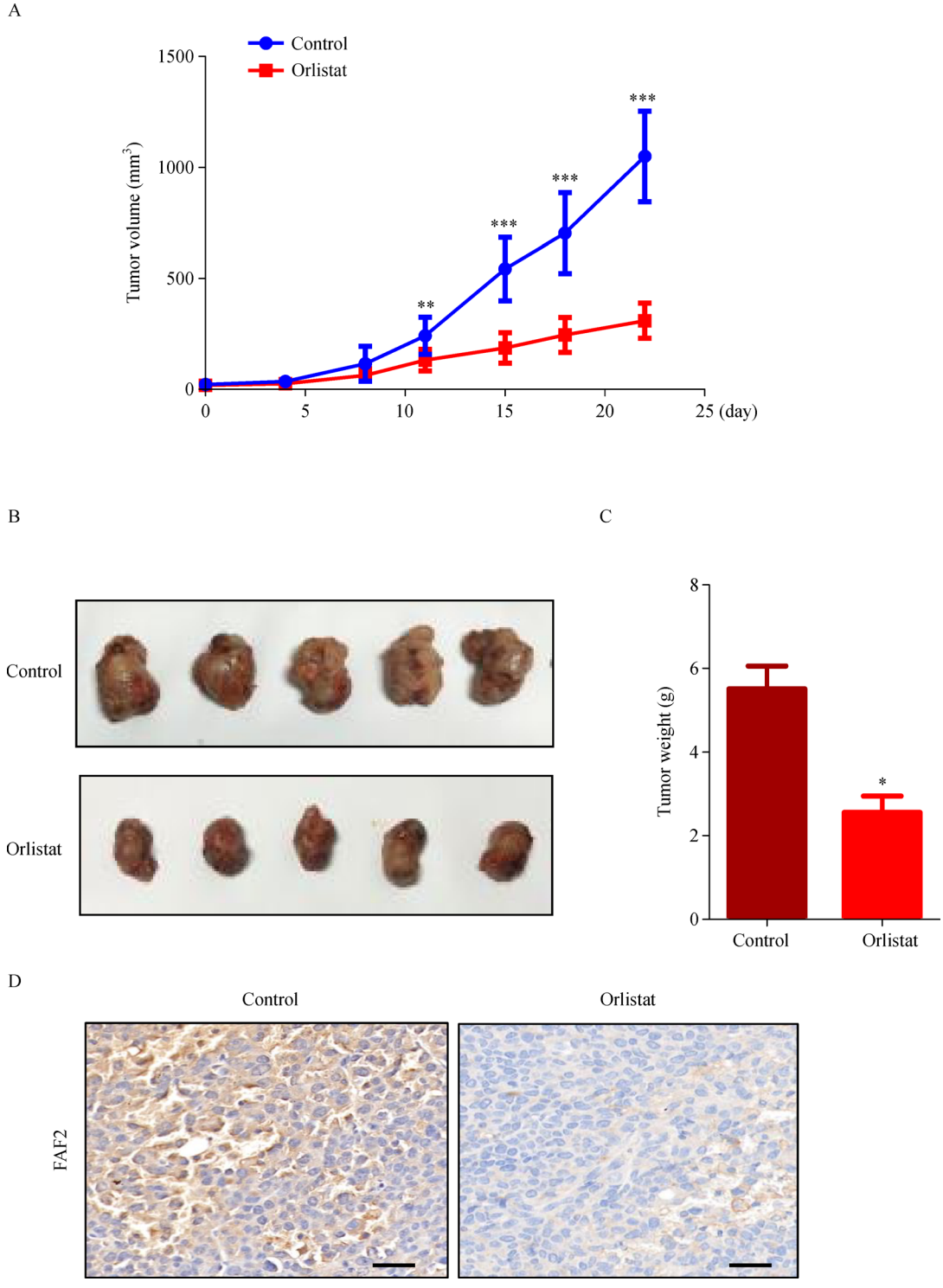

Fig. 6 Orlistat inhibited tumor growth *in vivo*. (A) Mice were treated with orlistat (10 mg/kg, i.p.) for 14 days, and tumor volumes were measured twice a week for 22 days. Data were represented as mean ± SEM (**$P < 0.01$, ***$P < 0.001$). (B) Real tumors from mice treated with orlistat or vehicle. (C) Tumor weights of mice from the treatment and control groups. Data were presented as mean ± SEM (*$P < 0.05$). (D) IHC staining of FAF2 in tumor tissues after treatment. Two representative images were presented to show FAF2 expression in tumor tissues treated with control or orlistat (scale bar = 50 μm).

Acknowledgements

This study was supported by grants from the National Natural Science Foundation of China (No. 81672314), the Key Natural Science Project of Anhui Provincial Education Department (No. KJ2020A1244, KJ2020A0578, and KJ2018A0221), and National Innovation Program for College Students (Nos. 201810367021 and 201710367036).

Compliance with ethics guidelines

Wenjing Zhou, Jing Zhang, Mingkun Yan, Jin Wu, Shuo Lian, Kang Sun, Baiqing Li, Jia Ma, Jun Xia, and Chaoqun Lian have declared no conflict of interest. The animal studies and procedures were approved by the Institutional Animal Care and Use Committee at Bengbu Medical College.

References

1. Bray F, Ferlay J, Soerjomataram I, Siegel RL, Torre LA, Jemal A. Global cancer statistics 2018: GLOBOCAN estimates of incidence and mortality worldwide for 36 cancers in 185 countries. CA Cancer J Clin 2018; 68(6): 394–424
2. Gouw AM, Eberlin LS, Margulis K, Sullivan DK, Toal GG, Tong L, Zare RN, Felsher DW. Oncogene KRAS activates fatty acid synthase, resulting in specific ERK and lipid signatures associated with lung adenocarcinoma. Proc Natl Acad Sci USA 2017; 114(17): 4300–4305
3. Lu C, Ma J, Cai D. Increased HAGLR expression promotes non-small cell lung cancer proliferation and invasion via enhanced *de novo* lipogenesis. Tumour Biol 2017; 39(4): 1010428317697574
4. Singh A, Ruiz C, Bhalla K, Haley JA, Li QK, Acquaah-Mensah G, Montal E, Sudini KR, Skoulidis F, Wistuba II II, Papadimitrakopoulou V, Heymach JV, Boros LG, Gabrielson E, Carretero J, Wong KK, Haley JD, Biswal S, Girnun GD. *De novo* lipogenesis represents a therapeutic target in mutant Kras non-small cell lung cancer. FASEB J 2018; 32(12): 7018 – 7027
5. Ali A, Levantini E, Teo JT, Goggi J, Clohessy JG, Wu CS, Chen L, Yang H, Krishnan I, Kocher O, Zhang J, Soo RA, Bhakoo K, Chin TM, Tenen DG. Fatty acid synthase mediates EGFR palmitoylation in EGFR mutated non-small cell lung cancer. EMBO Mol Med 2018; 10(3): e8313
6. Sayin VI, LeBoeuf SE, Papagiannakopoulos T. Targeting metabolic bottlenecks in lung cancer. Trends Cancer 2019; 5(8): 457–459
7. Drent ML, Larsson I, William-Olsson T, Quaade F, Czubayko F, von Bergmann K, Strobel W, Sjöström L, van der Veen EA. Orlistat (Ro 18-0647), a lipase inhibitor, in the treatment of human obesity: a multiple dose study. Int J Obes Relat Metab Disord 1995; 19(4): 221–226
8. Harp JB. Orlistat for the long-term treatment of obesity. Drugs Today (Barc) 1999; 35(2): 139–145
9. Schcolnik-Cabrera A, Chávez-Blanco A, Domínguez-Gómez G, Taja-Chayeb L, Morales-Barcenas R, Trejo-Becerril C, Perez-Cardenas E, Gonzalez-Fierro A, Dueñas-González A. Orlistat as a FASN inhibitor and multitargeted agent for cancer therapy. Expert Opin Investig Drugs 2018; 27(5): 475–489
10. Sokolowska E, Presler M, Goyke E, Milczarek R, Swierczynski J, Sledzinski T. Orlistat reduces proliferation and enhances apoptosis in human pancreatic cancer cells (PANC-1). Anticancer Res 2017; 37(11): 6321–6327
11. Xiao X, Liu H, Li X. Orlistat treatment induces apoptosis and arrests cell cycle in HSC-3 oral cancer cells. Microb Pathog 2017; 112: 15–19
12. Czumaj A, Zabielska J, Pakiet A, Mika A, Rostkowska O, Makarewicz W, Kobiela J, Sledzinski T, Stelmanska E. *In vivo* effectiveness of orlistat in the suppression of human colorectal cancer cell proliferation. Anticancer Res 2019; 39(7): 3815–3822
13. You BJ, Chen LY, Hsu PH, Sung PH, Hung YC, Lee HZ. Orlistat displays antitumor activity and enhances the efficacy of paclitaxel in human hepatoma Hep3B cells. Chem Res Toxicol 2019; 32(2): 255–264
14. de Almeida LY, Mariano FS, Bastos DC, Cavassani KA, Raphelson J, Mariano VS, Agostini M, Moreira FS, Coletta RD, Mattos-Graner RO, Graner E. The antimetastatic activity of orlistat is accompanied by an antitumoral immune response in mouse melanoma. Cancer Chemother Pharmacol 2020; 85(2): 321–330
15. Zhang C, Sheng L, Yuan M, Hu J, Meng Y, Wu Y, Chen L, Yu H, Li S, Zheng G, Qiu Z. Orlistat delays hepatocarcinogenesis in mice with hepatic co-activation of AKT and c-Met. Toxicol Appl Pharmacol 2020; 392: 114918
16. Cioccoloni G, Aquino A, Notarnicola M, Caruso MG, Bonmassar E, Zonfrillo M, Caporali S, Faraoni I, Villivà C, Fuggetta MP, Franzese O. Fatty acid synthase inhibitor orlistat impairs cell growth and down-regulates PD-L1 expression of a human T-cell leukemia line. J Chemother 2020; 32(1): 30–40
17. Drummen GP, van Liebergen LC, Op den Kamp JA, Post JA. C11-BODIPY(581/591), an oxidation-sensitive fluorescent lipid peroxidation probe: (micro)spectroscopic characterization and validation of methodology. Free Radic Biol Med 2002; 33(4): 473–490
18. Angeles TS, Hudkins RL. Recent advances in targeting the fatty acid biosynthetic pathway using fatty acid synthase inhibitors. Expert Opin Drug Discov 2016; 11(12): 1187–1199
19. Calderón Guzmán D, Hernández García E, Juárez Jacobo A, Segura Abarca L, Barragán Mejía G, Rodríguez Pérez R, Juárez Olguín H. Effect of orlistat on lipid peroxidation, Na^+, K^+ ATPase, glutathione and serotonin in rat brain. Proc West Pharmacol Soc 2011; 54: 73–77
20. Imai H, Matsuoka M, Kumagai T, Sakamoto T, Koumura T. Lipid peroxidation-dependent cell death regulated by GPx4 and ferroptosis. Curr Top Microbiol Immunol 2017; 403: 143–170
21. Yang WS, SriRamaratnam R, Welsch ME, Shimada K, Skouta R, Viswanathan VS, Cheah JH, Clemons PA, Shamji AF, Clish CB, Brown LM, Girotti AW, Cornish VW, Schreiber SL, Stockwell BR. Regulation of ferroptotic cancer cell death by GPX4. Cell 2014; 156 (1-2): 317–331
22. Wu J, Minikes AM, Gao M, Bian H, Li Y, Stockwell BR, Chen ZN, Jiang X. Intercellular interaction dictates cancer cell ferroptosis via NF2-YAP signalling. Nature 2019; 572(7769): 402–406
23. Poursaitidis I, Wang X, Crighton T, Labuschagne C, Mason D, Cramer SL, Triplett K, Roy R, Pardo OE, Seckl MJ, Rowlinson SW, Stone E, Lamb RF. Oncogene-selective sensitivity to synchronous cell death following modulation of the amino acid nutrient cystine. Cell Rep 2017; 18(11): 2547–2556
24. Li Y, Yang X, Yang J, Wang H, Wei W. An 11-gene-based prognostic signature for uveal melanoma metastasis based on gene expression and DNA methylation profile. J Cell Biochem 2019; 120: 8630–8639